MARIA WŁODARCZYK

Kielce University of Technology,
Al. Tysiąclecia Państwa Polskiego 7,
25-314 Kielce, Poland,
e-mail: mariaw@tu.kielce.pl

CRACKING PROCESS OF REINFORCED CONCRETE BEAMS IN FUNCTION OF BENDING MOMENT

Abstract

The results of performed test on reinforced concrete beams were treated as the basis for the further analysis. The beams differed only in the way of load application. Below the value of nominal cracking moments the growth of process intensity is very small and above it can be regarded as proportional to the bending moment. The process intensity λ for the beams subjected to live load comparing to the beams under monotonous load grows faster with the increasing load.

Keywords: bending moment, reinforced concrete beams

1. Introduction

The stochastic model of the process of crack formation and their calculation method in the reinforced concrete elements is described in the paper [1]. The distance between cracks was calculated assuming that close to the crack location loss of the adherence between concrete and steel occurs and stresses in concrete decrease. This excludes forming of a new crack on the left- (a_L) and right-side (a_P) of the developed crack. Using this model a computer programme to estimate the intensity of cracking process has been written [2].

In the paper an attempt to estimate relations between the intensity of cracking process and bending moment has been done. The results of performed test on reinforced concrete beams were treated as the basis for the further analysis. The beams differed only in the way of load application.

2. Description of the experiments

The experimental tests was performed on simply supported beams using the so-called four-point bending loading. There is a zone of pure bending in the beam tested. The section was monitored carefully for getting reliable data about strain localization and crack width for different levels of loading and unloading. In the following, a detailed description of examined reinforced concrete beams is given.

Two series of technically identical, reinforced concrete beams differently loaded were examined. The first series of examined beams consisted of four reinforced beams and the second series consisted of 13 beams. For all the tested beams the tension zone was reinforced with three bars ϕ12 made of steel 34GS, with mean yield strength of reinforcement f_{yk} = 435,23 MPa. In the compression zone two bars ϕ 8 made of steel St3S were used. For stirrups ϕ4,5 bars made of St3S steel were used. Between the applied forces 225 mm stirrup spacing, whereas 100 mm stirrup spacing at the supports was used.

Beams were made of concrete of identical recipe. Mean value of concrete compressive strength was estimated on the basis of experimental data and varied from f_{cm} = 22.08 MPa to f_{cm} = 29.56 MPa for each batches of concrete.

The beams of the first series (S1) were subjected to step growing load: 0 → 5 → 7,5 → 10 → 15 → 20 → 25 kN and so on, until collapse. The beams of second series (S2) were subjected to step live load with repeated unloading on higher load level: 0 → 5 → 7,5 → 10 → 0 → 10' → 15 → 0 → 15' → 20 → 0 → 20' → 25 kN and so on, till collapse. Load capacity force for beams ranged from 34.75 kN up to 38.75 kN.

For each loading and unloading analysed, on the surface of concrete at the level of tensile reinforcement, measurements of crack width and their location were carried out. The test results of two series of reinforced concrete beams were written into the data bases and were used for further analysis.

3. The results of research

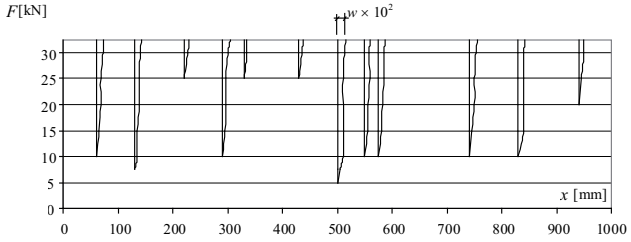

Fig. 1. Process of crack forming in S1B01 beam

Graphical method of presentation of the test results was used because of the size of digital data bases developed. The test results are illustrated, as an example, for S1B01 beam (Fig. 1) and for S2B01 beam (Fig. 2).

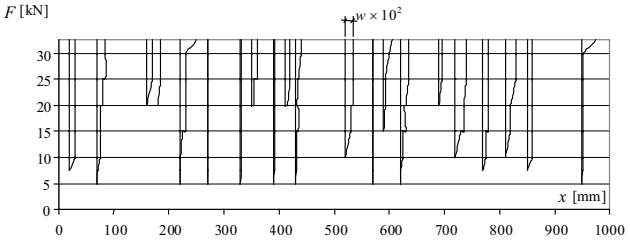

Fig. 2. Process of crack forming in S2B01 beam

Mean distances between cracks for each tested beams are given in the table 1.

Table 1. Mean, experimental distances between cracks

Beam	Mean distances between cracks x [mm] for tested beams on each level of load F [kN]												
	7,5	**10**	**10'**	**15**	**15'**	**20**	**20'**	**25**	**25'**	**30**	**30'**	**32.5**	**35**
S1B01	408	241	–	124	–	117	–	105	–	91	–	84	–
S1B02	261	190	–	128	–	108	–	93	–	85	–	–	80
S1B03	1000	426	–	317	–	175	–	140	–	96	–	88	84
S1B04	310	213	–	150	–	108	–	98	–	86	–	80	80
S2B01	1000	243	243	192	173	121	113	101	101	101	91	91	–
S2B02	-	512	512	205	205	249	249	181	181	149	140	133	26
S2B03	1000	174	179	110	088	82	75	64	64	64	64	63	–
S2B04	1000	476	227	122	116	78	68	66	64	60	60	60	–
S2B05	1000	255	289	224	146	108	85	76	73	71	71	–	–
S2B06	146	113	107	89	89	85	78	76	68	66	66	–	–
S2B07	1000	208	122	104	86	69	67	63	63	61	61	59	–
S2B08	194	164	118	89	85	85	85	85	82	79	79	–	–
S2B09	–	517	344	167	187	131	111	111	95	91	84	–	–
S2B10	1000	305	244	202	187	162	151	122	104	96	92	92	89
S2B11	–	511	633	156	137	115	115	109	99	91	87	70	70
S2B12	210	175	293	155	155	127	127	115	79	79	74	71	71
S2B13	–	–	507	197	181	151	141	132	85	85	85	85	–

4. The intensity of cracking process

In order to describe the intensity of cracking process λ the probabilistic model of crack formation proposed in [3] was used. The governing equation is:

$$\frac{\delta f_\lambda(\lambda,t)}{\delta\lambda} = \tag{1}$$

$$= \begin{cases} -f_\lambda(\lambda,t)\int_{2a}^{\infty} z_c f_\lambda(\lambda,t)dz & \text{for } t \le 2a \\ -f_\lambda(\lambda,t)\int_{2a}^{\infty} z_c f_\lambda(\lambda,t)dz + 2\int_{t+2a}^{\infty} f_\lambda(\lambda,t)dz & \text{for } a \le t < 2a \\ -f_\lambda(\lambda,t)\int_{2a}^{\infty} z_c f_\lambda(\lambda,t)dz + 2\int_{t+2a}^{\infty} f_\lambda(\lambda,t)dz - t_c f_\lambda(\lambda,t) & \text{for } t \ge 2a \end{cases}$$

where: a is the length of section where loss of adherence between concrete and reinforcement occurs, λ is the intensity of cracking process.

The solution of (1) was obtained numerically using programme LAMBDA [2] written for this purpose.

The length of adherence loss section a was estimated on the basis of the measured crack width and the value of stresses in reinforcement at the crack location:

$$a = \frac{wE_s}{2\sigma_{IIa}} \tag{2}$$

where: w is the width of crack, E_s is the elasticity modulus of reinforcement, and σ_{IIa} is the stress in reinforcement at the crack location.

In case of overlapping adherence loss sections (Fig. 3) the value of a was calculated using the following relation:

$$2a + x_l - x_k = \sum_{k=1}^{l} \frac{w_i E_s}{2\sigma_{IIa}} \tag{3}$$

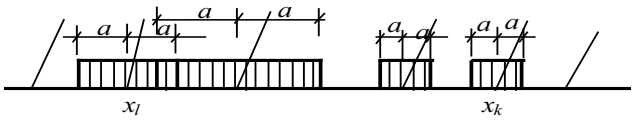

Fig. 3. Overlapping adherence loss sections

Since the process of calculation had to be repeated several times, where a is a variable, a tool programme ODCINEK_A [2] was developed.

Because of random character of adherence loss section the parameter a was defined as a random variable. The length of adherence loss section is then treated as an independent random variable for a given type of beam with probability density function $f_a(a)$ and mean value $E(a)$. As a result the following equation for random function is obtained:

$$f(x,\lambda) = \int_0^\infty f_a(a)\, f_\lambda(x|a)\, \mathrm{d}a \tag{4}$$

To calculate the random function with a treated as a random variable [3], programme ROZSTAW [2] was used. The result being the probability density functions $f(x,\lambda)$ are presented in Fig. 4, and relation between mean distances of cracks and the process intensity in Fig. 5.

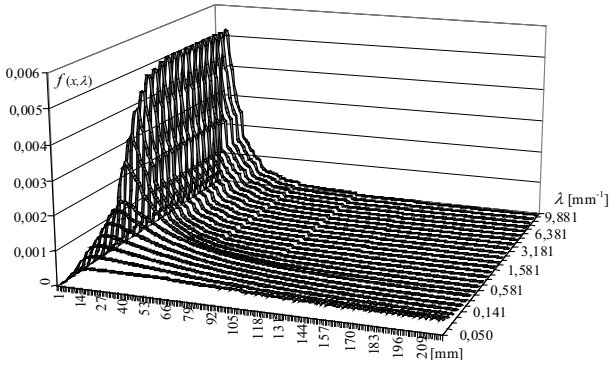

Fig. 4. Density function

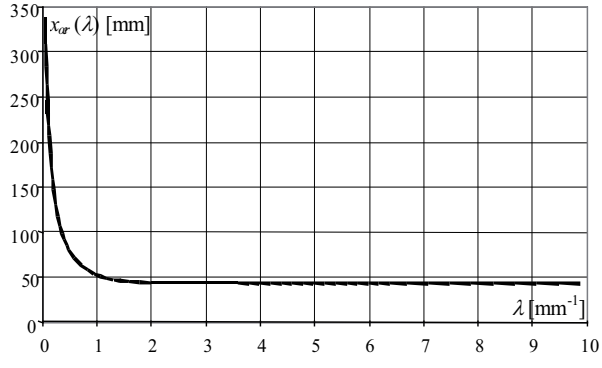

Fig. 5. Theoretical relationship between the mean distance of crack and the intensity process

5. Relationship between the intensity of crack process and bending moment

In order to determine the relation between the intensity process function λ and the bending moment mean theoretical values of crack distances have been adjusted to the experimental distances for each beam:

$$x_{sr,j}\left(M_j\right) = x_{sr}\left(\lambda_{i,j}\right) \tag{5}$$

where: i is the number of beam, j is the load number of load.

Hence, the empirical values of the function were estimated:

$$\lambda_{i,j} = \left(M_j\right) \tag{6}$$

and shown in Fig. 6.

For theoretical description the relation $\lambda(M)$ the polynomial function was applied. Polynomials up to third degree have been analysed in case of the monotonously and low–cyclically loaded beams.

Approximating function parameters have been determined using the least square method by minimizing the distance:

$$S^2 = \sum_{i=1}^{n}\sum_{j=1}^{m}\left[\lambda_{i,j} - \lambda_{i,j}\left(M_{i.j}\right)\right] \tag{7}$$

where: $\lambda_{i,j}$ is the value for beam i and load j.

Values determined from (7) are presented in the Table 2.

Since the deviation squares S^2 in case of linear or parabolic functions do not differ significantly, then, linear function can be accepted without loss of approximation accuracy. Finally, for linear approximating functions results are presented in Fig. 6.

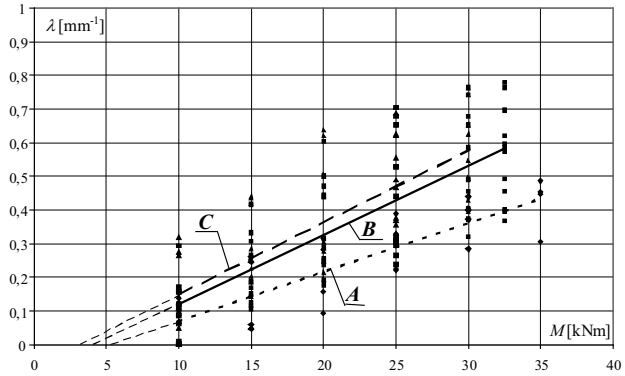

Fig. 6. Relationship $\lambda(M)$ for investigated beams

In Fig. 6 rhombuses mark quantities results for beams from the first series and a dotted line the corresponding approximation function ***A***. Square and triangle marks

Table 2. Approximating function parameters and deviations

Function	*a*	*b*	*c*	*d*	S^2
The first series (monotonic load)					
$\lambda(M) = aM+b$	0,0146	-0,0776	–	–	0,0005
$\lambda(M) = aM^2+bM+c$	-0,00009	0,0187	-0,1166	–	0,0003
$\lambda(M) = aM^3+bM^2+cM+d$	-0,00003	0,0001	0,0142	-0,0893	0,0016
Second series (primary load)					
$\lambda(M) = aM+b$	0,0204	-0,0839	–	–	0,0016
$\lambda(M) = aM^2+bM+c$	-0,0003	0,0345	-0,2134	–	0,0021
$\lambda(M) = aM^3+bM^2+cM+d$	0,000004	-0,0006	0,0390	-0,2399	0,0024
Second series (secondary load)					
$\lambda(M) = aM+b$	0,0215	-0,0686	–	–	0,0031
$\lambda(M) = aM^2+bM+c$	-0,0006	0,0442	-0,2674	–	0,0019
$\lambda(M) = aM^3+bM^2+cM+d$	-0,00004	0,0015	0,0051	-0,0462	0,0417

are given for the beams from the second series. For the path of the primary loading squares are used with a corresponding function marked with a solid line ***B***, whereas for the secondary loading path triangles are used with the corresponding broken line ***C***.

In the modelling, the cracking moment for the tested beams corresponds to the process intensity, for which mean crack distance is $x_{śr}$ = 1000 mm. Since the description of the process for large distances between cracks is almost identical with classic Poisson's process, the obtained value:

$$\lambda_{cr} \approx \frac{1}{x_{śr}} = \frac{1}{1000} \text{ [mm-1]}, \quad (8)$$

is close to zero. It can be accepted that the extrapolation of the lines (thin broken lines) until intersection with moment axis determine values of the nominal cracking moments:

$$M_{cr} = -\frac{b}{a} \quad (9)$$

Using (9) the value of nominal cracking moment for the beams in the first series is M_{cr} = 5,31 kNm. For the beams in the second series subjected to live load the value for the primary load path is M_{cr} = 4,11 kNm, and on the secondary load path is M_{cr} = 3,19 kNm.

Value of cracking moment calculated according to the norm [5] is equal to $M_{cr\,tot}$ = 9,36 kNm and is significantly higher not only than nominal cracking moments but also then ones observed during the tests (Table 1).

Comparing the quantities of nominal cracking moments it has been concluded that for the beams for the second series moments are smaller than for the first series. The lower values are the result of live load influence.

Analysing the relations $\lambda(M)$ (Fig. 6) the differences in the position of approximating functions are noticeable. The significant influence of live load on the increase in the process intensity is visible (lines ***B*** and ***C***) in relation to the monotonously loaded beams (line ***A***).

For live loads lines ***B*** and ***C*** are similar. Values $\lambda(M)$ for the secondary load (line ***C***) are above the values obtained on the increasing path, which is the result of cumulating influence of live loads.

The differences between ***B*** and ***C*** lines come from adding the effect of the last unload. These differences grow along with the unload value.

It has also been observed that the faster growth of process intensity begins above nominal cracking moments.

6. Conclusions

1. Below the value of nominal cracking moments the growth of process intensity is very small and above it can be regarded as proportional to the bending moment.
2. A significant influence of live load on quantities of nominal cracking moments has been observed.
3. The process intensity λ for the beams subjected to live load comparing to the beams under monotonous load grows faster with the increasing load.

References

[1] Goszczyński S., Goszczyńska B.: *Losowy proces tworzenia się rys w belkach żelbetowych*. Archiwum Inżynierii Lądowej, Tom XXVI 3 (1980), s. 603 – 620.

[2] Włodarczyk M.: *Zarysowanie zginanych belek żelbetowych jako proces stochastyczny*. Praca doktorska. Kielce 2002.

[3] Goszczyńska B.: *Losowy proces powstawania rys w strefie czystego zginania belek żelbetowych*. Praca doktorska. Kielce 1984.

[4] Goszczyński S., Włodarczyk M.: *Wpływ średnicy zbrojenia na wielkość odcinka utraty przyczepności*. XLVII Konferencja Naukowa KILiW PAN i KN PZITB, Krynica 2001, s. 83-90.

[5] PN-B-03264:2002, *Konstrukcje betonowe, żelbetowe i sprężone. Obliczenia statyczne i projektowanie.*

Maria Włodarczyk

Proces zarysowania belek żelbetowych w funkcji momentu zginającego

1. Wstęp

Stochastyczny model procesu powstawania rys w elementach żelbetowych oraz metodę ich obliczania został zaproponowany w pracy [1]. Obliczanie rozstawu rys oparto na założeniu, że w otoczeniu powstałej rysy następuje zerwanie przyczepności pomiędzy betonem i stalą oraz spadek naprężeń w betonie, co wyklucza powstanie nowej rysy w jej lewo- (a_L) i prawostronnym (a_P) otoczeniu. W prezentowanej pracy podjęto próbę oszacowania relacji między intensywnością procesu zarysowania i momentem zginającym.

2. Opis przeprowadzonych badań

Zbadano dwie serie, identycznych technicznie, belek żelbetowych różniących się między sobą sposobem realizacji obciążenia. Dla wszystkich zbadanych belek w strefie rozciąganej zastosowano trzy pręty ϕ12 ze stali 34GS o średniej granicy plastyczności f_{yk} = 435,23 MPa i w strefie ściskanej dwa pręty ϕ8 ze stali St3S. Belki wykonano z betonu o takiej samej recepturze. Średnia wytrzymałość określona na podstawie wyników badań wahała się od f_{cm} = 22,08 MPa do f_{cm} = 29,56 MPa dla poszczególnych zarobów.

Wszystkie badane belki były swobodnie podparte i obciążone dwoma siłami skupionymi w odległości l/3 od podpór. Pierwsza seria belek (S1) była poddana działaniu obciążenia skokowe, narastającego aż do zniszczenia. Natomiast drugą serię belek (S2) poddano działaniu obciążenia złożonego, które obejmowało skokowy wzrost siły z kilkukrotnymi odciążeniami. Siła niszcząca wahała się od 34,75 kN do 38,75 kN.

Na poszczególnych poziomach obciążenia i odciążenia wykonano między innymi pomiary szerokości rys oraz zinwentaryzowano ich położenie. Pomiary były prowadzone na powierzchni betonu w miejscu występowania zbrojenia rozciąganego.

3. Wyniki badań

Ze względu na duże rozmiary baz do prezentacji uzyskanych wyników zastosowano metody graficzne. Rezultaty uzyskane z badań poszczególnych belek zostały przykładowo zilustrowane wynikami dla belki S1B01 (rys. 1) i dla belki S2B01 (rys. 2).

4. Intensywność procesu zarysowania

W celu opisania intensywności procesu zarysowania λ wykorzystano zaproponowany w [1] probabilistyczny model powstawania rys. Rozwiązanie równania:

$$\frac{\delta f_{\lambda}(\lambda,t)}{\delta\lambda} = \tag{1}$$

$$= \begin{cases} -f_{\lambda}(\lambda,t)\int_{2a}^{\infty} z_c f_{\lambda}(\lambda,t)dz & \text{dla } t \le 2a \\ -f_{\lambda}(\lambda,t)\int_{2a}^{\infty} z_c f_{\lambda}(\lambda,t)dz + 2\int_{t+2a}^{\infty} f_{\lambda}(\lambda,t)dz & \text{dla } a \le t < 2a \\ -f_{\lambda}(\lambda,t)\int_{2a}^{\infty} z_c f_{\lambda}(\lambda,t)dz + 2\int_{t+2a}^{\infty} f_{\lambda}(\lambda,t)dz - t_c f_{\lambda}(\lambda,t) & \text{dla } t \ge 2a \end{cases}$$

gdzie: a – długość odcinka utraty przyczepności pomiędzy betonem i stalą, λ – intensywność procesu zarysowania.

Otrzymano na drodze numerycznej wykorzystując specjalnie napisany do tego celu program LAMBDA [2].

Długość odcinka utraty przyczepności a oszacowano na podstawie pomierzonej szerokości rysy i wielkości naprężeń w stali w przekroju przez rysę:

$$a = \frac{wE_s}{2\sigma_{IIa}} \tag{2}$$

gdzie: w – szerokość rysy, E_s – moduł sprężystości stali, σ_{IIa} – naprężenia w stali w przekroju przez rysę.

5. Zależność pomiędzy intensywnością procesu l a momentem zginającym

W celu wyznaczenia zależności pomiędzy intensywnością procesu λ a momentem zginającym porównano średnie teoretyczne wartości rozstawu rys z odległościami doświadczalnymi dla poszczególnych belek:

$$x_{śr,i}(M_j) = x_{śr}(\lambda_{i,j}) \tag{3}$$

gdzie: i – numer belki, j – numer obciążenia.

Na tej podstawie otrzymano empiryczne wartości funkcji

$$\lambda_{i,j}(M_j) \tag{4}$$

Celem uzyskania opisu teoretycznego przyjęto związek $\lambda(M)$ w formie funkcji wielomianowej.

6. Wnioski

1. Do umownych momentów rysujących wzrost intensywności procesu zarysowania jest bardzo mały, a powyżej można przyjąć, że jest proporcjonalny do momentu zginającego.
2. Stwierdzono znaczący wpływ obciążeń zmiennych na wielkości umownych momentów rysujących.
3. Intensywność procesu λ dla belek poddanych obciążeniu zmiennemu w porównaniu z belkami obciążonymi monotonicznie rośnie szybciej w miarę wzrostu obciążenia.